The Tetraspanin CD9 Affords High-Purity Capture of All Murine Hematopoietic Stem Cells

Göran Karlsson,[1] Emma Rörby,[2] Cristina Pina,[1,4] Shamit Soneji,[1,2] Kristian Reckzeh,[2] Kenichi Miharada,[2] Christine Karlsson,[2] Yanping Guo,[1] Cristina Fugazza,[1] Rajeev Gupta,[1] Joost H.A. Martens,[3] Hendrik G. Stunnenberg,[3] Stefan Karlsson,[2] and Tariq Enver[1,2,*]

[1]Stem Cell Laboratory, University College London Cancer Institute, London WC1E 6BT, UK
[2]Molecular Medicine and Gene Therapy, Lund Stem Cell Center, Lund University, 22184 Lund, Sweden
[3]Department of Molecular Biology, Nijmegen Centre for Molecular Life Sciences, Radboud University, 6500HB Nijmegen, the Netherlands
[4]Department of Haematology, National Health Service Blood and Transplant, University of Cambridge, Cambridge CB2 0PT, UK
*Correspondence: t.enver@ucl.ac.uk
http://dx.doi.org/10.1016/j.celrep.2013.07.020

SUMMARY

Prospective isolation is critical for understanding the cellular and molecular aspects of stem cell heterogeneity. Here, we identify the cell surface antigen CD9 as a positive marker that provides a simple alternative for hematopoietic stem cell isolation at high purity. Crucially, CD9 affords the capture of all hematopoietic stem cells in murine bone marrow in the absence of contaminating populations that lack authentic stem cell function. Using CD9 as a tool to subdivide hematopoietic stem-cell-containing populations, we provide evidence for heterogeneity at the cellular, functional, and molecular levels.

INTRODUCTION

The ability to prospectively isolate discrete hematopoietic cell fractions has afforded the identification and functional analysis of hematopoietic stem and progenitor cells, allowing for detailed descriptions of the hierarchical organization of the hematopoietic system as well as of the transcriptional programs regulating commitment steps. The resulting road map of hematopoiesis provides a platform for the description of malignant target cells and molecular regulation of leukemogenesis. However, isolation of hematopoietic cell fractions is an ongoing process of refinement at both the progenitor and stem cell levels (Balazs et al., 2006; Kiel et al., 2005; Ooi et al., 2009; Pronk et al., 2007).

Hematopoietic stem cells (HSCs) have been best characterized in murine bone marrow (BM) and are defined by their ability to self-renew and differentiate in a manner that can support the hematopoietic system throughout life. Cells with this capacity are generally referred to as long-term HSCs, which distinguishes them from the so-called short-term HSCs that possess limited self-renewal capacity and transient multilineage repopulation ability. The potential of HSCs is perhaps best demonstrated by the ability of at least a fraction of putative HSCs to reconstitute the entire hematopoietic system in single-cell transplants (Kiel

et al., 2005; Osawa et al., 1996). The most commonly used methods purifying these cells involve fluorescence-activated cell sorting (FACS), using antibody combinations against lineage markers, stem-cell antigen (Sca)-1, and c-kit (LSK) further subdivided by either Fms-like tyrosine kinase receptor 3 (Flt3) and CD34 ($LSK^{Flt3-CD34-}$) or Slam markers ($LSK^{CD48-CD150+}$) (Adolfsson et al., 2001, 2005; Kiel et al., 2005; Osawa et al., 1996; Yang et al., 2005). Alternative strategies based on physical attributes of HSCs have also been reported (Goodell et al., 1996). Regardless of purification strategy, considerable heterogeneity remains in the HSC compartment, including variations in reconstitution kinetics, lineage output, and self-renewal potential (Copley et al., 2012).

Despite the considerable benefit current strategies have had for our understanding of HSC biology and the recent advances to these protocols through the addition of positive markers like EPCR and ESAM-1 (Balazs et al., 2006; Ooi et al., 2009), the cellular basis for HSC heterogeneity is still unclear. More specifically, the extent to which this relates to the presence of contaminating non-HSCs within the putative HSC populations, relates to the existence of true functional variation within the HSC pool, or is due to stochastic transcriptional noise within functionally similar HSCs remains elusive. Resolving these matters would be greatly facilitated by capturing all HSCs in the marrow and analyzing their functional and molecular biology at both population and single-cell levels. To this end, herein we identify CD9 as a tool for such studies and dissect heterogeneity within the HSCs defined by CD9 expression.

RESULTS AND DISCUSSION

CD9 Is a Positive Marker that Simplifies Prospective Isolation of HSCs

By global gene expression profiling of a BM-derived multipotent hematopoietic progenitor cell line, we have previously identified CD9 as a candidate marker for primitive hematopoietic cells (Bruno et al., 2004). Analyses of primary cells are consistent with this notion, demonstrating the highest CD9 levels in the HSC fraction (Figure S1) and raising the possibility that CD9
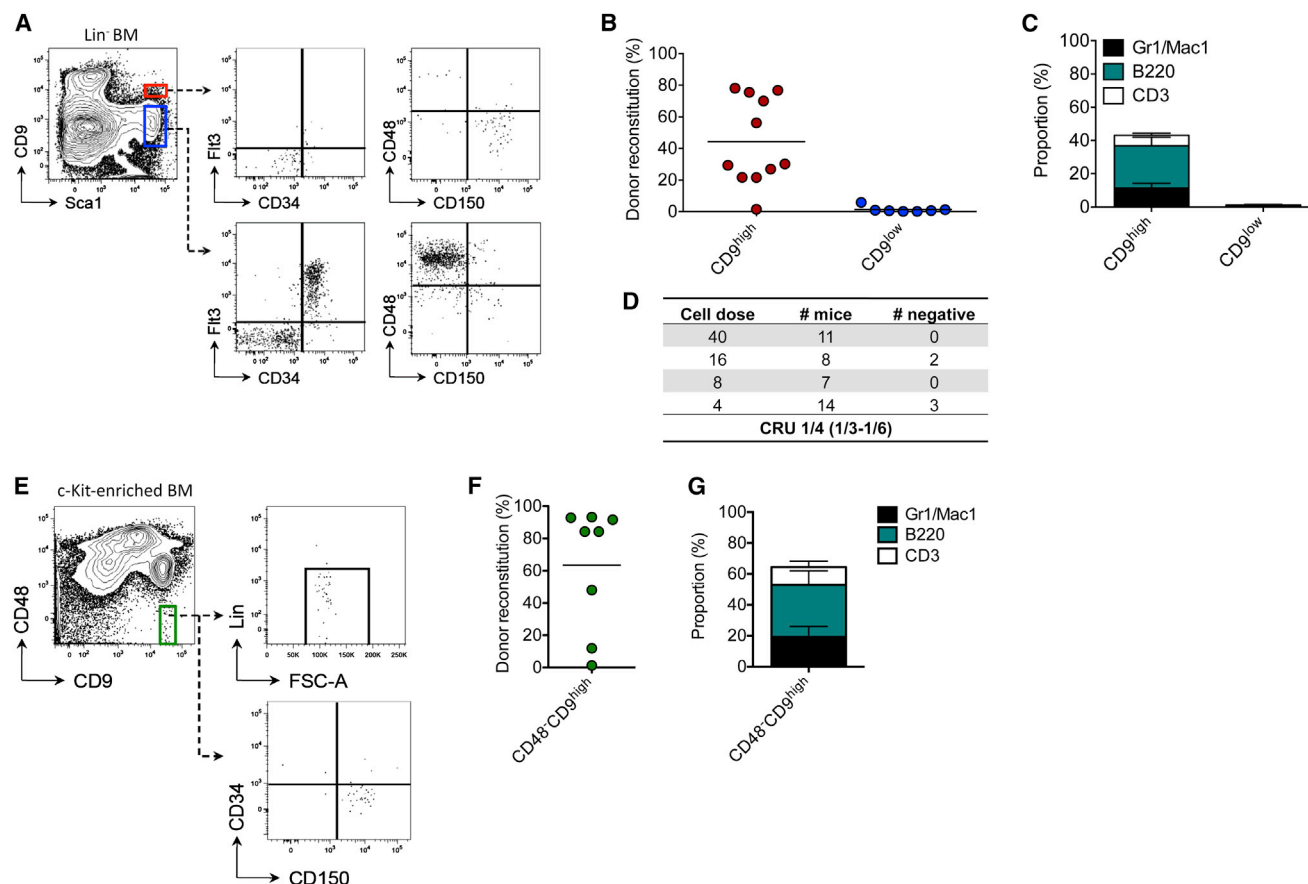
Figure 1. CD9 Allows for Simplified Purification of HSCs

(A) Sorting strategy and analysis for HSC markers of LS cells subdivided by CD9 expression.

(B and C) Donor contribution (B) and mean lineage distribution (C) in recipients transplanted with 40 CD9^{high} or 100 CD9^{low} LS cells. Each dot represents one recipient, n = 3.

(D) Estimation of CRU frequency in CD9^{high} LS cells based on limiting dilution transplantations using the indicated cell doses.

(E) Sorting strategy for CD48$^-$CD9^{high} cells and FACS analysis for HSC markers. In certain experiments, where c-kit enrichment is not as efficient, lineage depletion is necessary to achieve these results. It is, then, a simple matter to include a lineage cocktail in the CD48 channel.

(F and G) Donor contribution (F) and lineage distribution (G) in recipients transplanted with 20 CD48$^-$CD9^{high} cells.

See also Figures S1 and S4.

can be used for purification of HSCs. We therefore tested whether inclusion of CD9 as a positive selection marker could replace a number of other markers currently included in existing strategies, thereby simplifying prospective isolation of HSCs. Following lineage depletion and Sca-1 selection (LS) to exclude CD9-expressing progenitor populations (Figures S1 and S4), CD9^{high} cells showed an identical phenotype to HSCs isolated by the more complex existing strategies (Figure 1A; Table S1). Moreover, >90% of the CD9^{high} LS cells lacked intracellular expression of the proliferation marker Ki67, suggesting that they are in the quiescent, G$_0$ phase of the cell cycle, a documented trait of HSCs (Cheshier et al., 1999) (Figure S1). Of note, CD9^{high} cells read out as functional HSCs in transplantation assays and long-term reconstituting multiple hematopoietic lineages in primary recipients (Figures 1B and 1C), as well as over serial transplantation (data not shown). Limiting dilution transplantations further revealed similar HSC frequencies in the

CD9^{high} LS population as have been reported for populations purified by "conventional methods" (Kiel et al., 2005; Osawa et al., 1996) (Figure 1D). In contrast, CD9^{low} cells neither phenotypically nor functionally resemble HSCs. Taken together, our data demonstrate that CD9 can simplify prospective isolation of HSCs without loss of purity.

In deconstructing our strategy, we noted that further simplification could be made possible. C-kit enriched, CD48$^-$, CD9^{high} BM cells were negative for lineage markers and displayed an immunophenotypic HSC signature (Figure 1E). Additionally, low doses of CD48$^-$CD9^{high} cells gave robust long-term multilineage reconstitution in all recipients transplanted (Figures 1F and 1G), suggesting that HSCs could be isolated at high purity using only two channels.

In summary, CD9 significantly simplifies high-purity isolation of HSCs. This allows for HSC analysis when FACS or sorting possibilities are limited, as well as more advanced FACS analysis
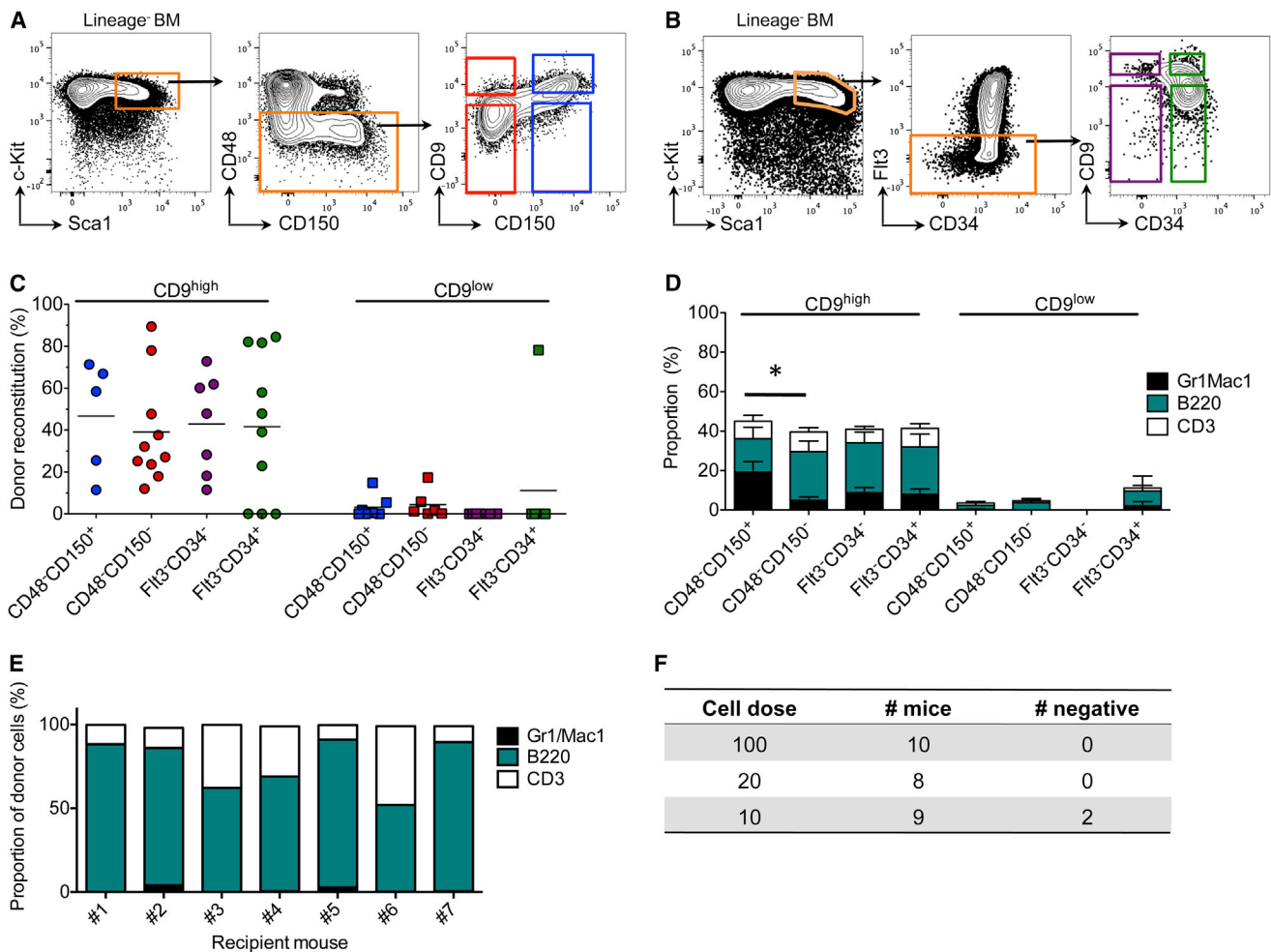
Figure 2. CD9 Captures All HSCs at High Purity and Is a Useful Tool for Exploring Their Functional Heterogeneity

(A and B) Representative plots for the sorting of HSC populations on the basis of LSK^{CD48CD150} (A) and LSK^{Flt3CD34} (B) staining further subdivided on the basis of CD9 expression.

(C) Sixteen-week donor contribution in recipients transplanted with HSCs purified with the indicated markers and subdivided based on expression of CD9. Each dot represents one recipient, and the graph illustrates data from two to four independent experiments.

(D) Mean lineage distribution in donor-derived peripheral blood presented in (C). Error bars represent SEM. The asterisk indicates a significant difference in reconstitution to the myeloid lineages (p < 0.05).

(E) Sixteen-week lineage distribution in recipients transplanted with 10 CD9^{high} LSK$^{CD48−CD150−}$ cells.

(F) Reconstitution frequencies in limiting dilution transplantations using CD9^{high} LSK$^{CD48−CD150−}$ cells at the indicated cell doses.

See also Figures S2 and S4.

on high-purity HSC populations, as three to four channels are freed for other markers.

CD9 Captures All HSCs in Murine BM

Stringent use of available markers already allows for high purity prospective isolation of HSCs. However, accumulating reports suggest that this comes at the expense of yield, and rare long-term reconstitution activity has been observed also in transplantation studies of both CD34$^+$ and CD150$^−$ populations (Challen et al., 2010; Osawa et al., 1996; Weksberg et al., 2008). We therefore asked whether CD9 could capture all HSCs in murine BM. To this end, we utilized CD9 to subdivide conventional populations known to contain HSCs and transplanted these into irradi-

ated recipient mice (Figures 2A, 2B, and S4; Table S1). The overlap between immunophenotypic HSC populations is presented in Figure S2. Interestingly, all HSC activity was detected in the CD9^{high} fractions, while no long-term engraftment to multiple lineages was detected in mice transplanted with CD9^{low} cells, except for in one outlier mouse (Figure 2C).

The capture of all HSCs at high purity further facilitates exploration of different aspects of HSC heterogeneity. Indeed, lineage distribution analysis indicated myeloid and lymphoid biases between CD150$^+$ and CD150$^−$ HSCs, respectively (Figure 2D). Specifically, lymphoid bias was detected in recipients transplanted with CD9^{high} LSK$^{CD48−CD150−}$ cells (Figure 2D). Our data suggest that this represents a self-renewing population
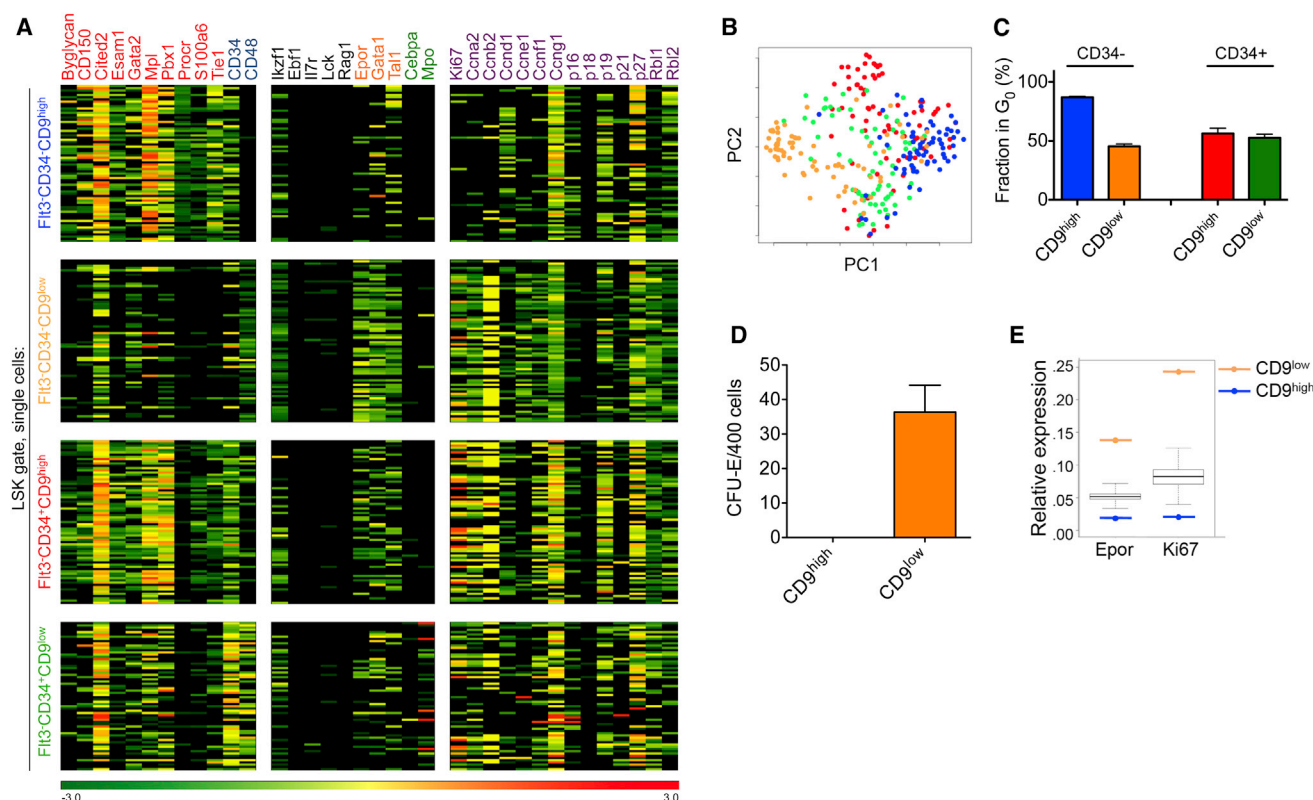
Figure 3. Single-Cell Transcriptional Profiling Reveals Cellular Heterogeneity within HSC Populations

(A) Single-cell gene expression analysis of CD9^{high} LSK$^{Flt3-CD34-}$ (n = 70) and LSK$^{Flt3-CD34+}$ (n = 72) cells, as well as CD9^{low} LSK$^{Flt3-CD34-}$ (n = 71) and LSK$^{Flt3-CD34+}$ (n = 65) cells. Each row represents one cell. Genes are color coded according to the category they represent. The data show color representation of the inverted standard score of change in cycle threshold values normalized to three reference genes (*Atp5a1*, *Hprt*, and *Actb*).

(B) PCA of the data presented in (A). Each dot represents a cell and is color coded based on its immunophenotype as indicated in (A).

(C) FACS analysis of intracellular Ki67 expression in LSK cells further subdivided as indicated (n = 2). Error bars represent SEM.

(D) Day 3 colony-forming assay for CFU-E potential of the LSK$^{Flt3-CD34-}$ population subdivided by CD9 (n = 2). Error bars represent SEM.

(E) Determination of the skew in expression means of Epor and Ki67 in HSCs. The mean of each gene in the LSK$^{Flt3-CD34-}$ HSC population was calculated based on randomly sampled CD9^{high} and CD9^{low} cells to a ratio of 2.6:1 and was repeated 1,000 times to draw a distribution (box plot) against which the means (colored lines) from the CD9-enriched populations could be compared. Expression levels are relative to the housekeeping genes.

See also Figure S3.

with a high frequency of lymphoid-biased cells since lineage skewing was maintained over serial transplants (Figure S2) and exacerbated when transplanting low doses of cells in limiting-dilution experiments (Figures 2E and 2F). Thus, CD9 is a useful tool for dissecting true functional HSC heterogeneity with respect to lineage bias within HSCs, a feature of HSCs that has recently come to the fore (Challen et al., 2010; Kent et al., 2009; Weksberg et al., 2008).

CD9 Affords Analysis of Molecular Heterogeneity in HSC Populations

CD9 allows for discrimination of bona fide HSCs from contaminating nonreconstituting cells within established HSC compartments, as well as capture of HSCs from cell fractions where they are thought to be rare. Thus the "conventionally sorted" long-term reconstituting HSC population (LSK$^{Flt3-CD34-}$) as well as the "conventional" short-term reconstituting HSCs (LSK$^{Flt3-CD34+}$) may be subdivided on the basis of CD9, yielding

four cell fractions with distinct immunophenotype and function. Having these at hand affords reinvestigation of transcriptional programs from different HSC fractions both at population level and at single-cell level. To this end, we performed single-cell quantitative multiplex reverse transcriptase (RT)-PCR analysis on a microfluidics-based platform for a preselected set of 36 genes documented as markers or functional regulators for HSCs, lineage commitment, or cell cycle (Figure 3A). The primary data (Figure 3A) and the principal-component analysis (PCA; Figure 3B) highlight not only the relationship between these different compartments but also the heterogeneity within them. An overwhelming proportion of cells from the CD9^{high} fraction of the long-term reconstituting HSC population (LSK$^{FLT3-CD34-}$) expressed HSC-related genes, while Ki67 and cyclins critical for cell cycle were silent. Of the lineage markers assayed, only scattered expression of megakaryocyte-erythroid genes was observed (Figure 3A). In contrast, expression of HSC genes was infrequent among CD9^{low} cells of this fraction, while Ki67
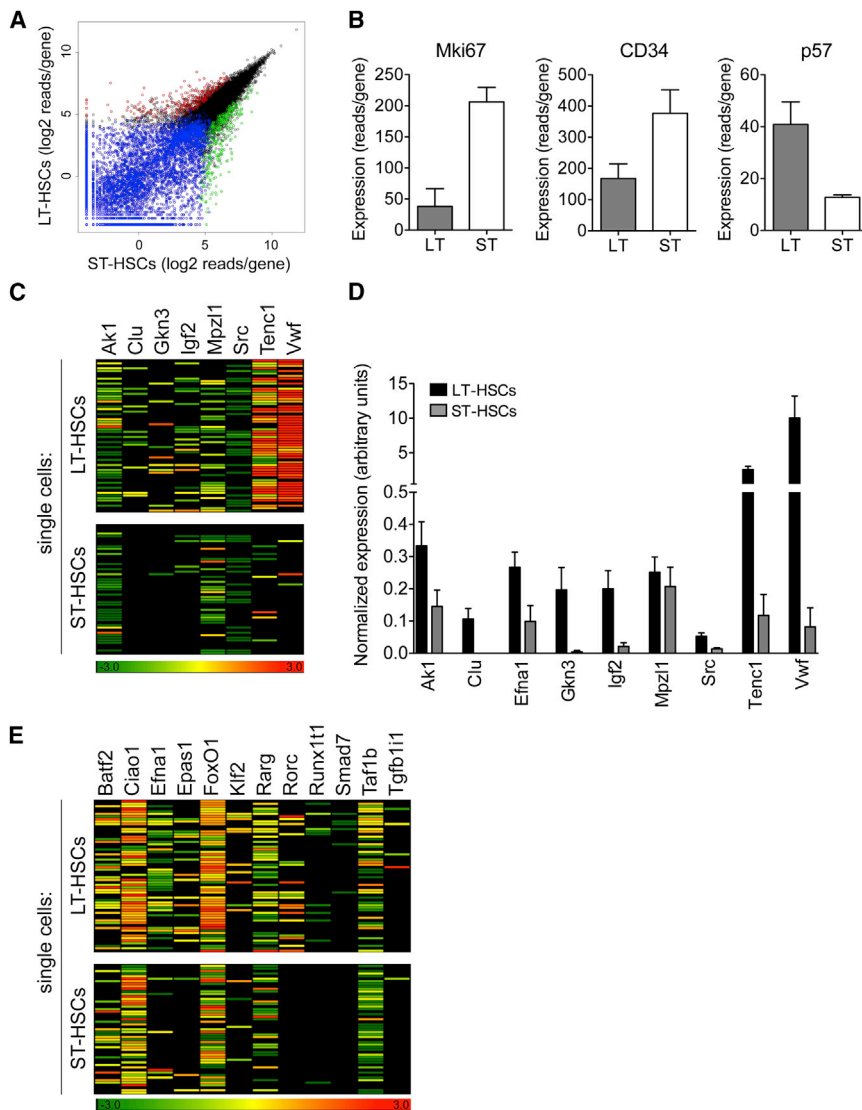
Figure 4. High-Resolution Global Gene Expression Analyses and Molecular Heterogeneity within Single HSCs

(A) Dot plot of RNA-seq analysis: blue dots represent genes that failed to pass quality filtering; red and green dots represent genes with more than 2-fold higher or lower expression in LT-HSCs, compared to ST-HSCs, respectively.

(B) RNA-seq data from genes expected to be deregulated between the LT- and ST-HSCs. Error bars represent SEM.

(C and D) Validation of the RNA-seq data by single-cell qPCR analysis of genes with varying upregulation in LT-HSCs presented at single-cell level (C) and as mean expression (D). Error bars represent SEM.

(E) Single-cell gene expression data of transcriptional regulators that were upregulated in LT-HSCs using both RNA-seq and qPCR analysis. The data in (C) and (E) show color representation of inverted standard score of ΔCT values normalized to three reference genes (*Atp5a1*, *Hprt*, and *Actb*).

See also Tables S2 and S3.

Our studies of CD9-enriched HSCs reveal a more transcriptionally coherent picture within HSCs than has been previously described (Månsson et al., 2007). PCA of the single-cell gene expression data reveal that 55/100 (1/1.8) LSK$^{FLT3-CD34-}$ cells share a similar HSC molecular signature (Figure 3B). CD9^{high} enrichment of this population purifies this signature to 1/1.3 cells (53/70). Of note, this exclusion of molecularly dissimilar non-HSCs has substantial effect on gene expression analysis at population level, exemplified by the 2.7- and 3.9-fold downregulation of *Epor* and *Ki67* expression, respectively, following further enrichment of HSCs by CD9 (Figure 3E).

Within the "conventionally sorted" short-term reconstituting HSC population (LSK$^{FLT3-CD34+}$), CD9^{high} cells had a transcriptional pattern similar to that of the HSCs described earlier (i.e., CD9^{high} LSK$^{FLT3-CD34-}$), with HSC-related genes frequently expressed. However, this population contains a substantial proportion of cells expressing genes involved in cell cycle progression. FACS analysis confirmed that a difference in Ki67 expression discriminated between the different populations, where >90% of CD9^{high} LSK$^{FLT3-CD34-}$ cells were Ki67$^-$, compared to only 50% of the other CD9^{high} HSC population, as well as the CD9^{low} cells (Figure 3C). Thus, CD9 identifies functional heterogeneity within the HSC population relating to cell cycle status and allows for resolution of a proliferating HSC population expressing the activation marker CD34 (Sato et al., 1999). Of note, the recently identified HSC marker EPCR (*Procr*) (Balazs et al., 2006) was infrequently expressed in this repopulating

and cyclins were upregulated. It is striking that, among the CD9^{low} cells, 61% (44/72) of the cells expressed erythropoietin receptor (*Epor*) and a large majority of the Epor$^+$ cells additionally expressed the two other erythroid regulators, *Scl/Tal1* and *Gata1*, while lacking messenger RNA (mRNA) for *Cd34* and *Mpl* (Figure S3). In support of the molecular data suggesting erythroid-lineage character, CD9^{low} cells generated late erythroid colony-forming units (CFU-Es), with efficiency close to that of prospectively isolated CFU-E cells (Figure 3D; data not shown) (Pronk et al., 2007), while displaying poor colony-forming capacity for other myeloid progenitors (Figure S3). Thus, single-cell molecular profiling supports our functional data in that HSCs are exclusively found in the CD9^{high} fraction of the HSC population. CD9^{low} cells represent a nonreconstituting, contaminating progenitor population with mainly erythroid potential. Thus, CD9 affords resolution of cell heterogeneity resulting from copurification of lineage-committed cells with bona fide HSCs.

compartment, suggesting discrepancy between CD9 and EPCR expression (Figure 3A).

Again, the CD9^{low} fraction of LSK$^{FLT3-CD34+}$ cells presented an entirely different transcriptional pattern than that of CD9^{high} cells, displaying a largely silent HSC signature, while myeloid-correlating genes such as *Mpo* and *Cebpa* are expressed at higher frequencies (Figure 3A).

Thus, it is clear that further separation based on CD9 expression discriminates transcriptional profiles that were previously merged (Månsson et al., 2007) and that most instances of detection of lineage-affiliated markers occur in CD9^{low} non-HSCs rather than in CD9^{high} HSCs. This is in line with our recent findings on individual cells from self-renewing cell lines where large-scale expression of lineage programs and self-renewal capacity were separated (Pina et al., 2012).

Taken together, the ability to discriminate authentic HSCs from nonreconstituting cells affords analysis of true molecular HSC signatures, without the confounding variable of contaminating cells. This elimination of cellular heterogeneity resulting from copurification of non-HSCs gives insight into the transcriptional programs underlying stem cell function and further uncovers functional heterogeneity within the HSC pool.

High-Resolution RNA-Seq Analysis of CD9^{high} HSCs Reveals Molecular Heterogeneity on a Single-Cell Level

The capacity to dissect heterogeneity prompts a reinvestigation of global gene expression programs of prospectively isolated HSCs. We therefore performed RNA sequencing (RNA-seq) analyses of a highly purified and functionally homogenous HSC population (LT-HSCs; LSK$^{CD48-CD150+CD34-CD9high}$), depleted of lymphoid- and cell-cycle-biased HSCs. We compared this transcriptome with that of a primitive progenitor population lacking HSCs, but with low-engrafting, short-term multilineage reconstituting activity in our transplantation experiments (ST-HSCs; LSK$^{CD48-CD150+CD9low}$; data not shown). In two independent experiments, approximately 55 × 10^6 reads were aligned to the mouse genome. A total of 9,152 genes survived quality control and were analyzed for differential expression between LT- and ST-HSCs (Figure 4A). Genes such as *Mki67*, *Cdkn1c (p57)*, and *CD34* displayed substantial differential expression as expected (Figure 4B), while gene set enrichment analysis revealed significant overrepresentation of cell cycle genes within the ST-HSC sample, confirming the success of LT-/ST-HSC expression profiling by RNA-seq despite the observed and expected close relation between the two populations analyzed. We compiled a refined stem cell signature by identifying genes with >2-fold differential expression between compartments in both experiments: 241 genes were found to be upregulated in LT-HSCs, while 353 had increased expression in ST-HSCs (Figure 4A; Tables S2 and S3). Of eight differentially expressed genes at a range of fold changes analyzed, seven were validated as differentially expressed and also by the single-cell RT-quantitative PCR (qPCR) method (Figures 4C and 4D). We used the Gene Ontology database to identify a total of 22 differential genes involved in regulation of transcription. Of these, 18 were selected for single-cell qPCR analysis to obtain a measure of transcriptional homogeneity among HSCs. It is interesting that, among the 11 genes identified as upregulated in LT-HSCs, two

distinct patterns of expression emerged. (1) Twenty-seven percent of genes were expressed in most cells in both populations, albeit at higher levels in the individual LT-HSCs (*Ciao1*, *Taf1b*, and *FoxO1*); (2) the remaining 73% changed in frequency, although not in level, indicating heterogeneous expression of a subset of transcripts (*Batf2*, *Epas1*, *Klf2*, *Rarg*, *Rorc*, *Runx1t1*, *Smad7*, and *Tgfb1i1*; Figure 4E). Thus, although LT-HSCs are nearly homogeneous in functional terms and share a similar transcriptional signature with several genes (e.g., *Vwf*, *Tenc*) uniquely expressed in virtually all LT-HSCs (Figures 3A and 4C), a snapshot view of transcription factor expression reveals striking molecular heterogeneity of a fraction of genes. Thus, even after depletion of non-HSC progenitors, there is still considerable transcriptional noise and fate priming within the functionally largely homogenous HSCs.

EXPERIMENTAL PROCEDURES

Mice

C57Bl/6 (CD45.2), congenic B6SJL (CD45.1), and C57Bl/6 × B6SJL (CD45.1/CD45.2) mice were kept in ventilated racks and given autoclaved food and water in the barrier facility at the Biomedical Center of Lund University. All animal experiments were approved by the Lund University Animal Ethical Committee.

FACS Analysis and Sorting

Peripheral blood, unfractionated BM, or magnetically c-kit-enriched BM from 9- to 16-week-old mice was stained in PBS/fetal calf serum (FCS), with combinations of antibodies listed in Table S1. For cell cycle analysis, BM stained with the desired antibody cocktail was fixed with paraformaldehyde (Sigma), permeabilized with Triton-X (Sigma), and then stained with Ki67 (BD Biosciences). Cells were sorted on a FACSAriaI cell sorter (BD Biosciences) or analyzed on a FACSCanto II (BD Biosciences) or a Gallios (Beckman Coulter) flow cytometer.

Colony Assays

A total of 60–400 cells were sorted into Iscove's modified Dulbecco's medium (Gibco) containing 5% FCS and transferred to 35 mm Petri dishes in methylcellulose medium (M3434; STEMCELL Technologies) supplemented with 100 U/ml penicillin and 100 μg/ml streptomycin. CFU-Es were scored 3 days following plating, and other colonies were scored at day 12.

Transplantation Assays

Purified cells were sorted at indicated doses and mixed with 2 × 10^5 unfractionated support BM cells from a congenic strain. The cell suspension was transplanted into the tail vein of lethally irradiated (900 cGy) recipients. If not stated, 20 cells per recipient were transplanted for LSK$^{CD48-150+}$, LSK$^{Flt3-CD34-}$, and CD48$^-$CD9^{high} populations; 100 cells per recipient were transplanted for CD9^{low} LS cells, LSK$^{CD48-150-}$, and LSK$^{Flt3-CD34+}$, and 40 cells per recipient were transplanted for CD9^{high} LS cells. In limiting dilution assays for the LS9^{high} or LSK CD48$^-$CD150$^-$ populations, a recipient mouse was considered to be reconstituted if donor chimerism was >0.1% for both the myeloid and lymphoid lineages or only the lymphoid lineages, respectively (Figure S1). Competitive repopulating unit (CRU) frequency was calculated on the basis of negative recipients using L-calc software (StemCell Technologies).

Single-Cell qPCR Analysis

Single cells were sorted into lysis buffer containing 0.4% NP40, deoxynucleoside triphosphates, dithiothreitol, and RNase OUT (Invitrogen) and snap frozen. On thawing, CellsDirect reaction mix containing SSIII/PlatinumTaq (CellsDirect One-Step RT_qPCR kit, no ROX, Invitrogen) and 48 TaqMan assays to a final dilution of 0.05× each were added to the cell lysate for RT-PCR preamplification and gene expression quantification according to previously published protocols (Pina et al., 2012).

RNA-Seq

RNA from 2,000 sorted cells was processed using the SMARTer cDNA synthesis kit (Clontech). End repair was performed on the resulting DNA using Klenow and T4 PNK. A 3′ protruding A base was generated using Taq polymerase, and adapters were ligated. The DNA was loaded on gel, and a band corresponding to ∼300 base pairs (bp) (chromatin immunoprecipitation fragment plus adapters) was excised. The DNA was isolated, amplified by PCR, and used for cluster generation on the Illumina 1G genome analyzer (Illumina, Inc). The 35 bp tags were mapped to the mm9 version of the mouse genome, and reads within exons were quantified using SeqMonk. Reads within exons belonging to a single gene were summed to give total gene expression. Gene expression values were normalized to per-10^6 tags and converted to $\log_2$. Fold changes were calculated between matched LT- and ST-HSC pairs. Genes were called differentially expressed when more than 2-fold upregulated or downregulated in both paired sets. For Gene Set Enrichment Analysis (GSEA) (Subramanian et al., 2005), genes were ranked by fold change and imported into the GSEA v2.0 software, against which classes from the Gene Ontology were tested.

ACCESSION NUMBERS

The RNA-seq data have been deposited in the NCBI Gene Expression Omnibus (GEO) (http://ncbi.nlm.nih.gov/geo) and can be found at accession number GSE47707.

SUPPLEMENTAL INFORMATION

Supplemental Information includes four figures and three tables and can be found with this article online at http://dx.doi.org/10.1016/j.celrep.2013.07.020.

REFERENCES

Adolfsson, J., Borge, O.J., Bryder, D., Theilgaard-Mönch, K., Astrand-Grundström, I., Sitnicka, E., Sasaki, Y., and Jacobsen, S.E. (2001). Upregulation of Flt3 expression within the bone marrow Lin(-)Sca1(+)c-kit(+) stem cell compartment is accompanied by loss of self-renewal capacity. Immunity 15, 659–669.

Adolfsson, J., Månsson, R., Buza-Vidas, N., Hultquist, A., Liuba, K., Jensen, C.T., Bryder, D., Yang, L., Borge, O.J., Thoren, L.A., et al. (2005). Identification of Flt3+ lympho-myeloid stem cells lacking erythro-megakaryocytic potential a revised road map for adult blood lineage commitment. Cell 121, 295–306.

Balazs, A.B., Fabian, A.J., Esmon, C.T., and Mulligan, R.C. (2006). Endothelial protein C receptor (CD201) explicitly identifies hematopoietic stem cells in murine bone marrow. Blood 107, 2317–2321.

Bruno, L., Hoffmann, R., McBlane, F., Brown, J., Gupta, R., Joshi, C., Pearson, S., Seidl, T., Heyworth, C., and Enver, T. (2004). Molecular signatures of self-renewal, differentiation, and lineage choice in multipotential hemopoietic progenitor cells in vitro. Mol. Cell. Biol. 24, 741–756.

Challen, G.A., Boles, N.C., Chambers, S.M., and Goodell, M.A. (2010). Distinct hematopoietic stem cell subtypes are differentially regulated by TGF-beta1. Cell Stem Cell 6, 265–278.

Cheshier, S.H., Morrison, S.J., Liao, X., and Weissman, I.L. (1999). In vivo proliferation and cell cycle kinetics of long-term self-renewing hematopoietic stem cells. Proc. Natl. Acad. Sci. USA 96, 3120–3125.

Copley, M.R., Beer, P.A., and Eaves, C.J. (2012). Hematopoietic stem cell heterogeneity takes center stage. Cell Stem Cell 10, 690–697.

Goodell, M.A., Brose, K., Paradis, G., Conner, A.S., and Mulligan, R.C. (1996). Isolation and functional properties of murine hematopoietic stem cells that are replicating in vivo. J. Exp. Med. 183, 1797–1806.

Kent, D.G., Copley, M.R., Benz, C., Wöhrer, S., Dykstra, B.J., Ma, E., Cheyne, J., Zhao, Y., Bowie, M.B., Zhao, Y., et al. (2009). Prospective isolation and molecular characterization of hematopoietic stem cells with durable self-renewal potential. Blood 113, 6342–6350.

Kiel, M.J., Yilmaz, O.H., Iwashita, T., Yilmaz, O.H., Terhorst, C., and Morrison, S.J. (2005). SLAM family receptors distinguish hematopoietic stem and progenitor cells and reveal endothelial niches for stem cells. Cell 121, 1109–1121.

Månsson, R., Hultquist, A., Luc, S., Yang, L., Anderson, K., Kharazi, S., Al-Hashmi, S., Liuba, K., Thorén, L., Adolfsson, J., et al. (2007). Molecular evidence for hierarchical transcriptional lineage priming in fetal and adult stem cells and multipotent progenitors. Immunity 26, 407–419.

Ooi, A.G., Karsunky, H., Majeti, R., Butz, S., Vestweber, D., Ishida, T., Quertermous, T., Weissman, I.L., and Forsberg, E.C. (2009). The adhesion molecule esam1 is a novel hematopoietic stem cell marker. Stem Cells 27, 653–661.

Osawa, M., Hanada, K., Hamada, H., and Nakauchi, H. (1996). Long-term lymphohematopoietic reconstitution by a single CD34-low/negative hematopoietic stem cell. Science 273, 242–245.

Pina, C., Fugazza, C., Tipping, A.J., Brown, J., Soneji, S., Teles, J., Peterson, C., and Enver, T. (2012). Inferring rules of lineage commitment in haematopoiesis. Nat. Cell Biol. 14, 287–294.

Pronk, C.J., Rossi, D.J., Månsson, R., Attema, J.L., Norddahl, G.L., Chan, C.K., Sigvardsson, M., Weissman, I.L., and Bryder, D. (2007). Elucidation of the phenotypic, functional, and molecular topography of a myeloerythroid progenitor cell hierarchy. Cell Stem Cell 1, 428–442.

Sato, T., Laver, J.H., and Ogawa, M. (1999). Reversible expression of CD34 by murine hematopoietic stem cells. Blood 94, 2548–2554.

Subramanian, A., Tamayo, P., Mootha, V.K., Mukherjee, S., Ebert, B.L., Gillette, M.A., Paulovich, A., Pomeroy, S.L., Golub, T.R., Lander, E.S., and Mesirov, J.P. (2005). Gene set enrichment analysis: a knowledge-based approach for interpreting genome-wide expression profiles. Proc. Natl. Acad. Sci. USA 102, 15545–15550.

Weksberg, D.C., Chambers, S.M., Boles, N.C., and Goodell, M.A. (2008). CD150- side population cells represent a functionally distinct population of long-term hematopoietic stem cells. Blood 111, 2444–2451.

Yang, L., Bryder, D., Adolfsson, J., Nygren, J., Månsson, R., Sigvardsson, M., and Jacobsen, S.E. (2005). Identification of Lin(-)Sca1(+)kit(+)CD34(+)Flt3-short-term hematopoietic stem cells capable of rapidly reconstituting and rescuing myeloablated transplant recipients. Blood 105, 2717–2723.